ELSEVIER

Journal of Alloys and Compounds 446–447 (2007) 114–120

Journal of ALLOYS AND COMPOUNDS

www.elsevier.com/locate/jallcom

Nanostructured Mg–Mm–Ni hydrogen storage alloy: Structure–properties relationship

S. Løken [a,b], J.K. Solberg [b], J.P. Maehlen [a], R.V. Denys [a], M.V. Lototsky [a], B.P. Tarasov [c], V.A. Yartys [a,b,*]

[a] *Institute for Energy Technology, Kjeller NO 2027, Norway*
[b] *Norwegian University of Science and Technology, Trondheim NO 7491, Norway*
[c] *Institute of Problems of Chemical Physics of RAS, Chernogolovka 142434, Russia*

Received 30 October 2006; received in revised form 24 November 2006; accepted 28 November 2006
Available online 29 December 2006

Abstract

Kinetics of H uptake/release in Mg can be improved by alloying with Ni and RE, as well as by reducing the grain size of the Mg alloy. Both these approaches were applied in the present work for the alloy 72 wt.% Mg–20 wt.% Ni–8 wt.% Mm (ternary eutectic Mg–Mg_2Ni–$MmMg_{12}$). The alloy was processed by the equal channel angular pressing (ECAP) technique. In ECAP the sample is subjected to heavy plastic strain by pressing it through a die with an angle of 90°. ECAP treatment resulted in a fine microstructure compared to the rather heterogeneous as-cast material. Hydrogenated and non-hydrogenated samples were investigated using SEM and XRD. Hydrogenation properties were studied by TDS and PCT. Hydrogenated samples consist of MgH_2, Mg_2NiH_4 and MmH_{2+x} and exhibit a maximum H-storage capacity of ~5.5 wt.%. To initiate the first hydrogenation, the alloy needs to be activated at ~300 °C. However, already after one hydrogenation cycle its H-absorption becomes quite fast: 4.5 wt.% H is absorbed in just 15 min. Vacuum TDS (heating rate 0.5 °C/min) shows that desorption starts at low temperature, ~135 °C, with a peak at ~210 °C. The alloy was also subjected to high energy ball milling (HEBM) in Ar or H_2 to yield further refinement of the microstructure. ~1 wt.% Nb_2O_5 was added to facilitate H exchange. The H sorption characteristics of the alloy treated by ECAP and HEBM have been compared with the ones for the as-cast material.

Keywords: Hydrogen absorbing materials; Gas–solid reactions; Diffusion; X-ray diffraction

1. Introduction

Magnesium and magnesium-based alloys are very important materials for hydrogen storage applications. Pure magnesium can reversibly store up to 7.6 wt.% hydrogen in the form of MgH_2. Compared to other solid state hydrogen storage materials magnesium also has such advantages as low cost and large abundance in the earth's crust. However, slow hydrogen absorption and desorption kinetics, and high working temperatures above 250 °C are the disadvantages to overcome before practical use of magnesium as a hydrogen storage material will be possible. The high temperature needed is caused by slow reaction kinetics and high stability of MgH_2, having an enthalpy of formation $\Delta H^\circ = -74.7$ kJ/mol and an equilibrium dissociation hydrogen pressure of 1 atm at 285 °C.

However, magnesium and magnesium-based alloys fail to fulfil a goal of high rates of H charge/discharge at temperatures below 150 °C. Therefore practical use of Mg for hydrogen storage becomes problematic. Hydrogenation kinetics is related to the dissociation of molecular hydrogen at the metal surface and the diffusion of atomic hydrogen into the metal. The dissociation ability of Mg for hydrogen molecules is low, and the diffusion of atomic hydrogen in Mg (hydride) is very slow. It is therefore important to add catalytic materials and refine the metal microstructure to improve hydrogenation and dehydrogenation kinetics in order to make magnesium a suitable material for hydrogen storage applications. Alloying Mg with transition rare-earth elements and nickel is one of the approaches employed to improve the reaction thermodynamics

* Corresponding author at: Institute for Energy Technology, Kjeller, NO 2027, Norway. Tel.: +47 63 80 64 53; fax: +47 63 81 29 05.
E-mail address: volodymyr.yartys@ife.no (V.A. Yartys).

0925-8388/$ – see front matter © 2006 Elsevier B.V. All rights reserved.
doi:10.1016/j.jallcom.2006.11.200

and kinetics. Refining the microstructure of the alloy (i.e. grain size, intermetallic particle size) by rapid solidification, severe plastic deformation like equal channel angular pressing and mechanical milling, and adding catalysts like different types of oxides, have also been successfully used to improve the hydrogenation kinetics [1–3]. Barkhordarian et al. [4], and Hanada et al. [5] improved the hydrogen sorption kinetics of magnesium by adding metal oxide through mechanical milling. Specially Nb_2O_5 showed a very good effect on the sorption kinetics, both on absorption and desorption of hydrogen. An oxide content of as low as 0.2 mol% was enough to achieve both fast absorption and desorption kinetics [4,5].

In the present work we have studied the eutectic composition 72 wt.% Mg–20 wt.% Ni–8 wt.% Mm as hydrogen storage material. The work was focused on the effect of different metal productions routes on the hydrogen storage performance of this alloy. The following routes were applied: equal channel angular pressing (ECAP); high energy ball milling (HEBM) in argon and in hydrogen gas media; doping with a transition metal oxide catalyst, Nb_2O_5.

2. Experimental

The Mg–Mm–Ni alloy of composition 72 wt.% (88 at.%) magnesium, 20 wt.% (10 at.%) nickel and 8 wt.% (2 at.%) lanthanum rich Mischmetal has been prepared from high purity compact metal pieces by melting under protective atmosphere in an electrical resistance furnace. The melt was cast into a cylindrical rod in a copper chill with inner surface covered with boron nitride. Specimens for ECAP were machined from the cylindrical rod to dimensions 2 cm × 2 cm × 8 cm with the longest dimension oriented along the cylinder axis.

Equal channel angular pressing was carried out in a die with an angle between the two channels of 90° and an outer curvature of 20°. The die was made of Orvar Supreme tool steel and had a maximum working temperature of 550 °C [6]. Magnesium is a brittle material at room temperature so ECAP had to be done at higher temperatures. Pressing at 350 °C resulted in big cracks in the sample rod, but it was possible to do several pressings for each sample rod at 400 and 450 °C. Lubrication of the sample rods was necessary to lower the friction between the sample and the inner walls of the channels during pressing. A graphite-based lubricant (OMEGA99®) was used for lubrication. Pressing of the sample was executed immediately after reaching the set point temperature. After pressing, the sample was taken out of the die and quenched in water.

Both as-cast and ECAPed specimens were included in the experimental programme. In a preliminary test programme, several specimens were ECAPed according to a series of ECAP routes. Two of these samples were chosen for further investigation; i.e. a sample that was pressed two times using route B_c at 400 °C, later referred to as 2× ECAP, and a sample that was pressed eight times using route B_c at 400 °C, later referred to as 8× ECAP (route B_c: specimen is rotated 90° between successive presses). These two samples were chosen because they gave the most promising results after ECAP, i.e. the finest microstructure.

The hydrogen absorption–desorption studies were conducted in a conventional Sieverts-type apparatus. Determinations of hydrogen storage capacity and reaction kinetics by Sieverts method are done by measuring the pressure change in a closed system with a constant volume. Prior to hydrogenation, the sample was crushed to a particle size of about 10–100 μm in a mortar. As an activation process the sample was heated in vacuum (10^{-3} Pa) to 350 °C and kept at this temperature for 1 h. Then the sample was cooled to the wanted temperature, and hydrogen gas was admitted till the pressure reached 15–20 bar. Temperature desorption spectroscopy (TDS) was applied to determine the onset temperature for hydrogen release during dehydrogenation. Both during TDS and desorption in a closed volume, the heating of the sample was done at a constant heating rate of 0.5 °C/min until the sample temperature reached 350 °C.

HEBM was carried out in a SPEX 8000 D mixer mill and a Fritsch P6 planetary mill. Milling in the SPEX 8000 D mixer mill was performed in an argon atmosphere for 10 h with a ball to powder ratio of 10:1. Milling in the Fritsch P6 planetary mill was performed in a 40–50 bar H_2 atmosphere for 30 min, 1 h and 2 h. To avoid oxidation, samples were handled in a glove box under protective argon atmosphere.

The Johnson–Mehl–Avrami (JMA) [7] equation was used for kinetic evaluation of the absorption and desorption curves: $f = 1 - \exp[-(kt)^n]$, where f is fraction transformed; n a constant defining the rate limiting process; k rate constant; t is time.

X-ray diffraction (XRD) was used to characterize the phases present in the alloy before hydrogenation, as a hydride and after dehydrogenation. The powder pattern obtained by the XRD-measurements, using Siemens D5000 diffractometer equipped with a Ge primary monocromator giving Cu $K\alpha_1$ radiation, were refined by the Rietveld refinements with the GSAS program [8].

Scanning electron microscope (Hitachi S-4300SE field emission SEM) equipped with an Oxford Instrument Energy Dispersive X-ray spectrometer (EDX) was used to record images and measure chemical composition of the powder particles before hydrogenation, in charged condition and after dehydrogenation.

3. Results and discussion

SEM invesigation including EDX analysis showed that Mg–Mm–Ni alloy was a ternary eutectic alloy with two intermetallic phases, Mg_2Ni and $MmMg_{12}$, embedded in a matrix of pure Mg. The as-cast material was inhomogeneous with prevailing areas of coarse microstructure and much less areas of very fine microstructure. An area with a coarse microstructure in the as-cast alloy is shown in Fig. 1.

The phase composition of the alloy was confirmed by a Rietveld refinement of the XRD data (Fig. 2): ∼49 wt.% Mg, sp.gr. $P6_3/mmc$ (No. 194), $a = 3.2084(1)$ Å, $c = 5.2078(2)$ Å; ∼36 wt.% Mg_2Ni, sp.gr. $P6_222$ (No. 180), $a = 5.2111(2)$ Å, $c = 13.2491(3)$ Å; and ∼15 wt.% $MmMg_{12}$, sp.gr. $I4/mmm$ (No. 139), $a = 10.315(3)$ Å, $c = 5.952(2)$ Å. These data are in good agreement with a ternary phase diagram of the Mg–La–Ni system [9].

Processing of the alloy by ECAP at 400 °C gave a significant reduction of the particle sizes in the areas with originally coarse microstructure and resulted in a much more homogeneous material. During this treatment, the lamellae structure of as-cast alloy vanished, and spherical intermetallic particles appear instead. The most distinct effect on the microstructure was observed after

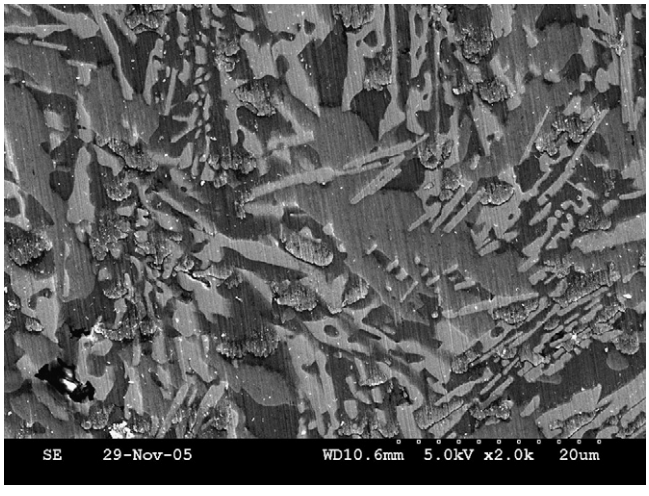

Fig. 1. SEM image of as-cast alloy showing coarse microstructure.

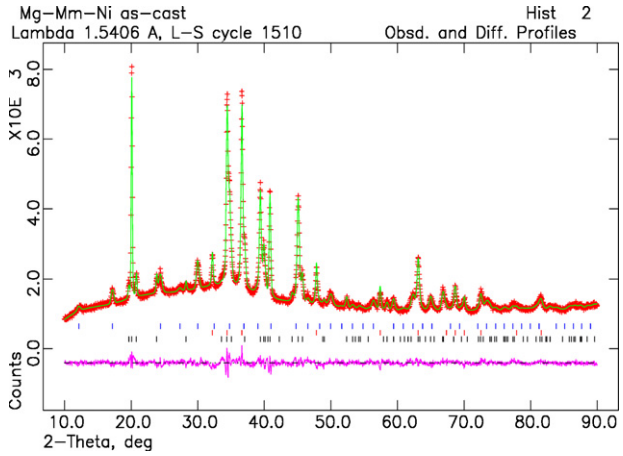

Fig. 2. XRD pattern of Mg–Mm–Ni as-cast alloy (Cu Kα). Bragg peaks from constituent phases are shown (top to bottom): Mg_2Ni (35.8(2) wt.%), Mg (48.9(2) wt.%), $MmMg_{12}$ (15.2(1) wt.%). *R*-values: $R_p = 3.12\%$, $R_{wp} = 3.83\%$; $\chi^2 = 2.16$. Mg: sp.gr. $P6_3/mmc$; $a = 3.20840(9)$; $c = 5.2078(2)$ Å; Mg_2Ni: sp.gr. $P6_322$; $a = 5.2111(2)$; $c = 13.2491(3)$ Å; $MmMg_{12}$: sp.gr. $I4/mmm$; $a = 10.315(3)$; $c = 5.952(2)$ Å. *Note*: for Mg and Mg_2Ni preferred orientation along [0 0 1] is observed.

eight passes of ECAP, see Fig. 3. No changes in phase composition of the alloy was found after the ECAP treatment. ECAP also increased the hardness of the alloy, due to either the smaller particle size, a higher dislocation density, a smaller Mg matrix grain size, or a combination of all these factors. Dislocations and grain/phase boundaries act as diffusion paths for hydrogen, so a harder metal, i.e. a metal with more dislocation and/or larger area of grain/phase boundaries, should provide better hydrogen diffusion properties.

HEBM of as-cast and ECAP treated samples for 10 h in Ar resulted in a reduction of the powder particle size. XRD showed a large difference in phase crystallinity before and after HEBM, an increased amount of amorphous structure was present after HEBM. The microstructure of the 2× ECAP alloy after HEBM is shown in Fig. 4. The light intermetallic particles are Mg_2Ni-phase, and the grey area is Mg matrix containing $MmMg_{12}$-phase. There has been a distinct refinement of the microstructure

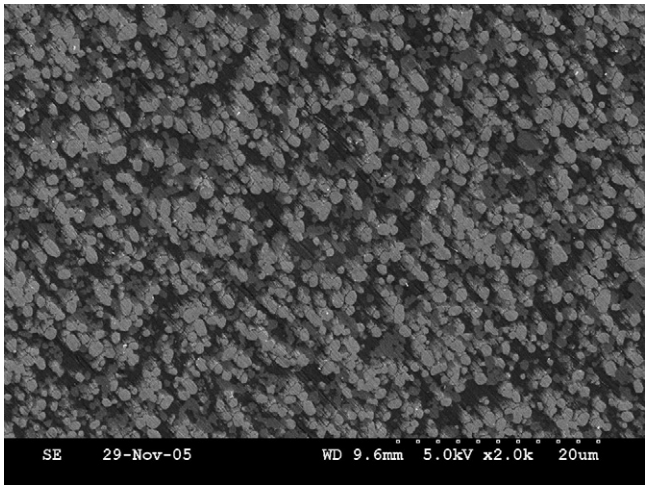

Fig. 3. Microstructure of the alloy after eight presses at 400 °C (8× ECAP).

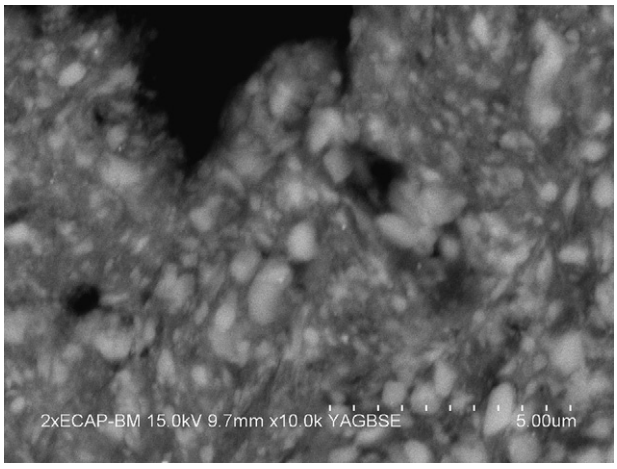

Fig. 4. Microstructure of the alloy after 2× ECAP and HEBM in Ar for 10 h.

due to HEBM. After HEBM it is very hard to distinguish the $MmMg_{12}$-phase from the Mg matrix. However, the light Mg_2Ni particles can easily be observed. The particle size of this phase becomes very small, from 150 nm and up to ∼1 μm.

Hydrogen sorption cycling at 325 °C of the as-cast, 2× and 8× ECAP alloy required at least five full absorption cycles before the alloy was activated. For all three samples, the first hydrogen absorption was very slow, and it took about 20 h to reach complete saturation. After full activation, the 8× ECAP alloy showed higher H-absorption and desorption rates than the as-cast alloy and the 2× ECAP alloy, see Table 1 and Fig. 5a. Fig. 5 shows absorption and desorption curves for fully activated specimens that had either not been ball milled, Fig. 5a, or ball milled with and without Nb_2O_5 additions, Fig. 5b. The activation properties were significantly improved after HEBM. After 10 h of HEBM in Ar, only one absorption cycle was required before the alloy was activated, and the 8× ECAP material had no longer a faster hydrogen sorption rate than other samples. For the 2× ECAP material, the ball milling increased the absorption and desorption rates with as much as up to three times.

This means that 10 h of HEBM gave a microstructure that is more refined than after 8× ECAP. The effect of ECAP at 400 °C is of little or no value compared to the HEBM. The intermetallic

Table 1
A comparison of hydrogen absorption and desorption rates of Mg–Mm–Ni after different production treatments and full activation

Material	Time (min)		
	To absorb 4 wt.% H	To absorb 4.5 wt.% H	To desorb ∼5 wt% H
As-cast	7.5	11	24
As-cast + BM	2.5	5.3	8
As-cast + BM with 1 wt.% Nb_2O_5	4.2	15.8	11
2× ECAP	9.5	14	∼30
2× ECAP + BM	2.5	6.3	∼7
2× ECAP + BM with 1 wt.% Nb_2O_5	4.0	12.7	∼10
2× ECAP + BM with 3 wt.% Nb_2O_5	3.8	10.6	∼8
8× ECAP	5	7.5	19
8× ECAP + BM	4.5	15.5	11
8× ECAP + BM with 1 wt.% Nb_2O_5	4.5	12.2	14

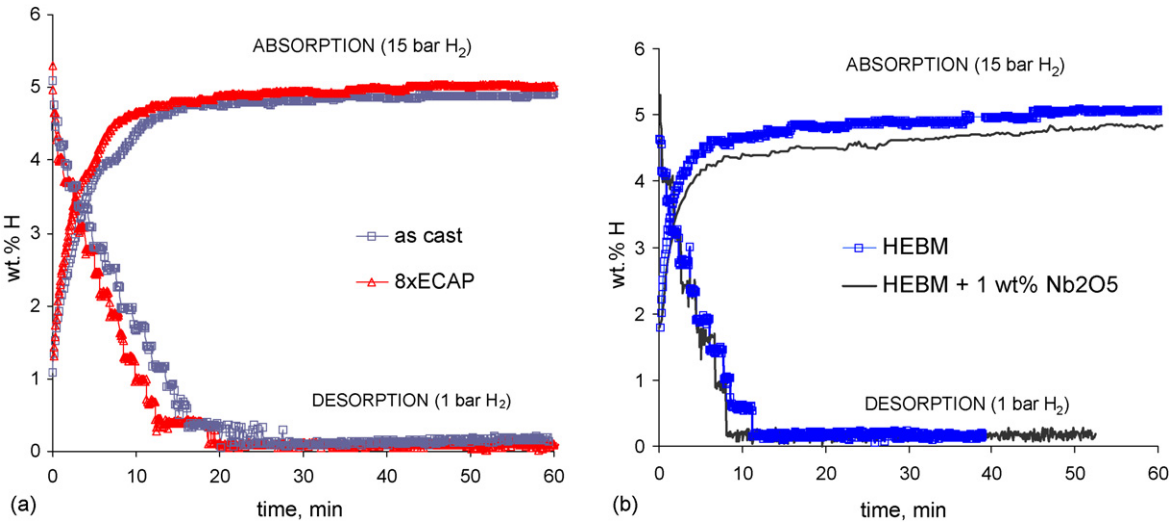

Fig. 5. Hydrogen absorption and desorption curves for fully activated samples of (a) as-cast and 8× ECAP material without ball milling and (b) 2× ECAP material ball milled in argon with and without Nb_2O_5 addition.

particle size is much smaller after HEBM than after ECAP and provides better diffusion paths for hydrogen atoms. The intermetallic particle sizes ranges from 0.15 to 1.0 μm after HEBM, which is about three times less than those after ECAP. Thus, the total effect of HEBM is a refinement of the intermetallic particle sizes that is stronger than for ECAP at 400 °C, in addition to a refinement of the powder itself, which gives a larger total area for the dissociation reaction of the hydrogen gas.

Adding oxides during HEBM did not give a further increase in the hydrogen absorption and desorption rates. Earlier studies have demonstrated superior both hydrogen absorption and desorption rates when adding Nb_2O_5 to magnesium and magnesium–nickel alloys. The results in this work show no positive effect of adding Nb_2O_5 to the alloy. In fact, the hydrogen absorption and desorption rate are lower for the samples ball milled with Nb_2O_5, Fig. 5b. This was unexpected, because added oxides have been reported to increase the absorption rate by as much as 4 times and desorption rate as much as 10 times [10]. But those studies were done on Mg and Mg/Mg_2Ni alloys and not on alloys that originally contained rare-earth elements or Mm. The catalytic effect of Nb_2O_5 and Mm is mainly on the dissociation of H gas. An explanation for no extra catalytic effect of Nb_2O_5 could be that Mm has already introduced this effect to the alloy. This shows the superior effect that Mm gives to Mg alloys on hydrogen absorption–desorption properties. All studied samples exhibited a hydrogen storage capacity of about 5.5 wt%.

For all samples, irrespectively of treatment, hydrogenation resulted in a formation of MgH_2, Mg_2NiH_4 and Mm-based hydride. The latter hydride was formed during decomposition of $MmMg_{12}$ to form MmH_{3-x} and MgH_2. Fig. 6 shows XRD pattern of Mm–Mg–Ni as-cast alloy hydrogenated after 16 absorption–desorption cycles. The desorbed material contained Mg, Mg_2Ni and MmH_2, which is a highly stable hydride below 600–700 °C. The quantitative analysis of the amount of phase constituents prior to and after the hydrogenation showed a good correspondence in the data for different samples. An increase of the MgH_2/Mg weight ratio from the initial ∼50/50 to ∼60/40 is in line with the process of the irreversible decomposition of $MmMg_{12}$ on hydrogenation producing extra MgH_2. SEM studies of the alloy after the hydrogenation cycles confirmed the presence of very small particles with high concentration of Mm in the microstructure. The particle size of the Mm-containing phases was measured to be from 10 to 100 nm.

HEBM in hydrogen gives an even more significant effect. Milling of the Mg–Mm–Ni alloy under 40 bar H_2 for 0.5–2 h resulted in almost complete hydrogenation of the alloy during the first cycle with formation of a nanocrystalline mixture of MgH_2, Mg_2NiH_4 and $Mg_2NiH_{0.3}$.

Pressure composition temperature (PCT) dependencies obtained for the 2× ECAP sample are shown in Fig. 7. Two plateaus are visible, the lower plateau corresponds to the

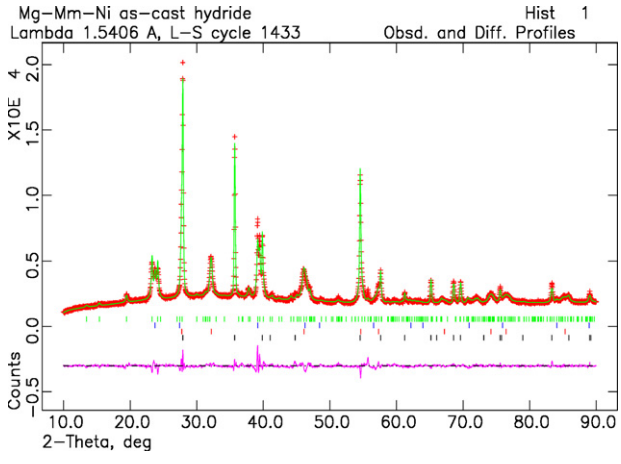

Fig. 6. XRD pattern of Mg–Mm–Ni as-cast alloy hydrogenated after 16 absorption–desorption cycles (Cu Kα). Bragg peaks from constituent phases are shown (top to bottom): Mg_2NiH_4 (low-temperature modification; sp.gr. $C2/c$; $a = 14.409(2)$; $b = 6.4285(8)$; $c = 6.5036(8)$ Å, $\beta = 113.662(8)°$), 31.4(2) wt.%; Mg_2NiH_4 (high-temperature modification, sp.gr. $Fm\bar{3}m$; $a = 6.4999(7)$ Å), 5.8(1) wt.%; MmH_{3-x} (sp.gr. $Fm\bar{3}m$; $a = 5.5709(2)$ Å), 8.8(1) wt.%; MgH_2 (sp.gr. $P4_2/mnm$; $a = 4.5254(6)$; $c = 3.02684(6)$ Å), 54.0(3) wt.%. R-values: $R_p = 3.99\%$, $R_{wp} = 5.77\%$; $\chi^2 = 4.1$.

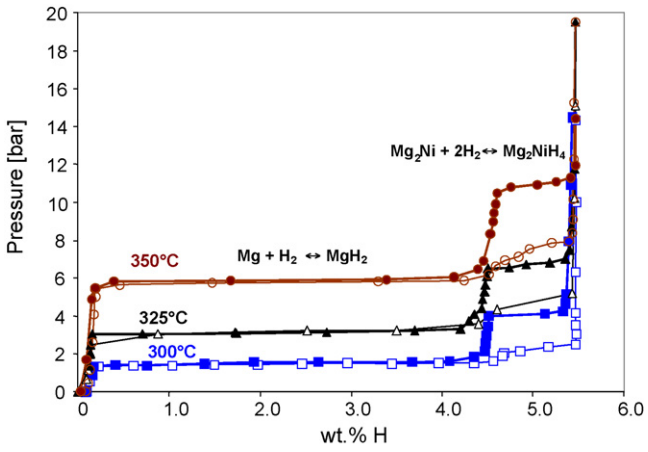

Fig. 7. PCT diagram for Mg–Mm–Ni processed with ECAP, two presses applying route B_c at 400 °C.

transformation $Mg \leftrightarrow MgH_2$, and the upper plateau belongs to the transformation $Mg_2Ni \leftrightarrow Mg_2NiH_4$ [11]. Enthalpy and entropy changes for the formation and decomposition of Mg- and Mg_2Ni-hydrides calculated from the van't Hoff plots [12] are shown in Table 2. The Mg-plateau pressure has not changed after 2× ECAP. Appearance of a large hysteresis and a slope in the upper Mg_2Ni-plateau, as well as the absence of discontinuities between the Mg- and Mg_2Ni-plateaus are observed after the ECAP treatment. Such effect of ECAP was also reported in the work by Skripnyuk et al. [2]. Also HEBM treatment normally leads to an increase in both slope and hysteresis for the Mg_2Ni-based hydride [3]. The obtained ΔH and ΔS values correspond well with literature values for Mg/Mg_2Ni alloy processed by ECAP [2]. The values for the MgH_2 hydride are in good agreement with the literature data for pure Mg and also for a Mg alloy (ZK60) processed by ECAP and HEBM [3].

Table 2
Thermodynamic and kinetic parameters for hydrogen absorption (desorption) of Mg and Mg_2Ni phases in Mg–Mm–Ni alloy

Value	Mg	Mg_2Ni
ΔH (kJ/mol H_2)	−78.9 (82.1)	−58.3 (70.8)
ΔS (J/(mol H_2 K))	141.2 (−146.5)	113.4 (−130.5)
n (300 °C)	0.55 (0.51)	0.82 (0.64)
k (300 °C) (h^{-1})	8.93 (10.99)	0.07 (0.66)
n (350 °C)	0.55 (0.50)	0.76 (0.88)
k (350 °C) (h^{-1})	5.64 (18.80)	0.18 (0.29)

The PCT-measurements also gave separate absorption curves for the MgH_2- and the Mg_2NiH_4-phase. Fig. 8 shows absorption and desorption curves obtained from selected PCT measurement data points at the respective plateaus for the two hydrides MgH_2 and Mg_2NiH_4. The differences between the curves are very similar for both absorption and desorption. The reaction rate for the MgH_2-phase is much faster than for the Mg_2NiH_4-phase. Mg-hydride reaches equilibrium after about one hour, while Mg_2Ni-hydride reaches equilibrium after 15–20 h. For both phases, there is a good fit with the JMA equation as shown in the graphs. Kinetic calculations showed that the rate constants for formation and decomposition of Mg_2NiH_4 are 50–150 times lower than those for MgH_2. Calculated n- and k-values of the JMA equation for both MgH_2 and Mg_2NiH_4 hydride are given in Table 2. There is a minor difference in the n-value identifying the rate-limiting process of the two hydrides. The Mg_2NiH_4-phase has an n-value of about 0.8, and the MgH_2-phase has an n-value of about 0.5. An n-value of 0.5 indicates that the rate-limiting process is diffusion controlled one-dimensional growth. For Mg_2NiH_4, diffusion is not only the rate limiting parameter, but by far the most important one.

Furthermore, there were also observed different values of the kinetic constants given in the JMA equation describing the absorption and desorption curves of the Mg–Mm–Ni alloy. The JMA equation was only able to fit the experimental data up to about 80–90% of the total storage capacity for the full absorption cycles. This indicates that the kinetics drastically changes after absorption of ∼4.5–4.9 wt.% hydrogen. The upper plateau of the PCT-isotherms starts at ∼4.5 wt.% H, so the reason why the JMA

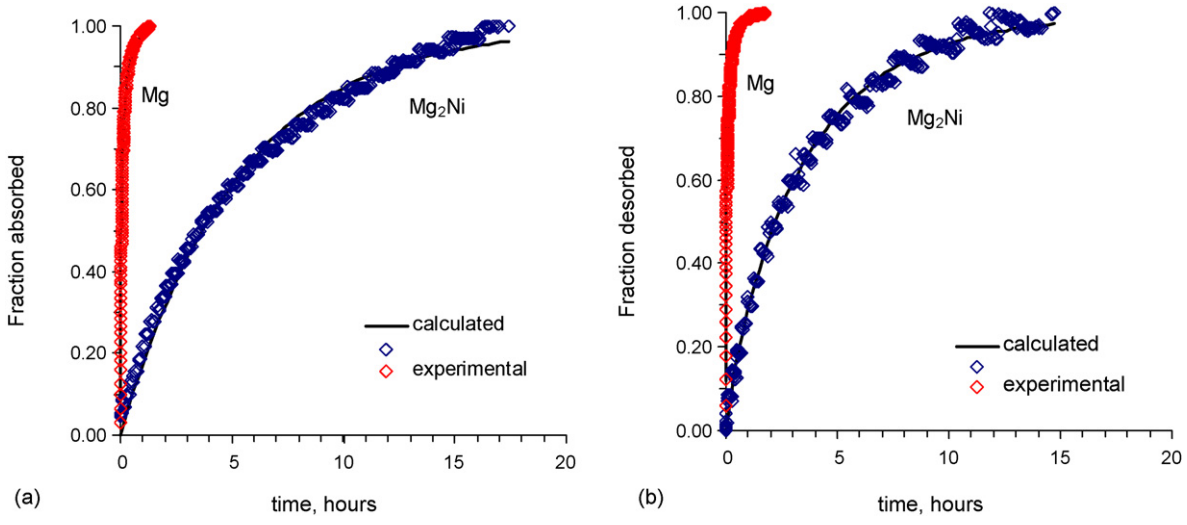

Fig. 8. Absorption (a) and desorption (b) curves for Mg and Mg_2Ni phases in the 2× ECAP Mg–Mm–Ni sample obtained in the plateau regions of the PCT diagram in Fig. 7.

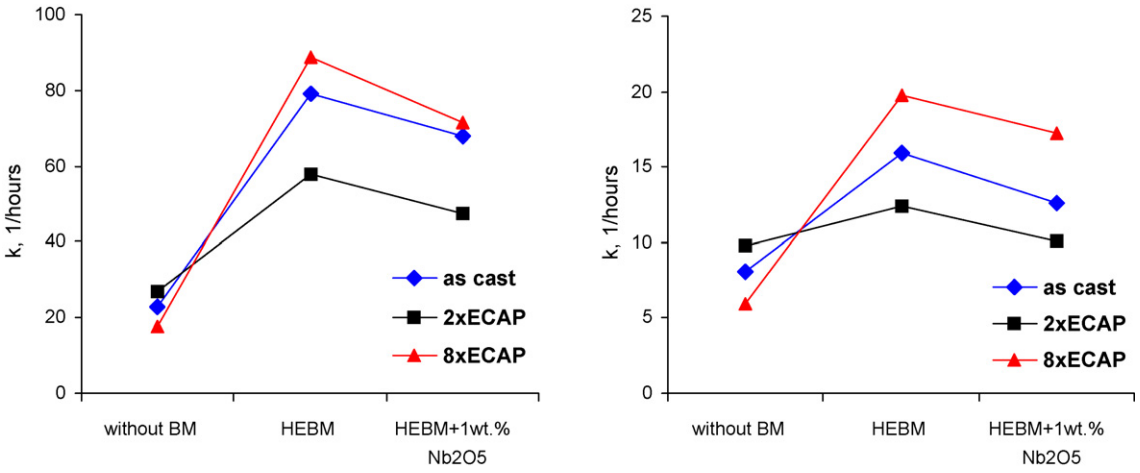

Fig. 9. Reaction rate constants for hydrogen absorption (a) and desorption (b) after different treatments.

equation fits only the first 80–90% of the absorption cycle can be that the fast absorption reaction of MgH_2 and the slow absorption reaction for Mg_2NiH_4 cannot be described by the same mechanism (similar *n*- and/or *k*-values). Desorption curves, however, could be fitted up to full desorption. An explanation for this can be that the difference in desorption equilibrium pressure between the two hydrides MgH_2 and Mg_2NiH_4 is small. The difference in the calculated *n*-values for desorption was also small for decomposition of the Mg and Mg_2Ni hydrides. The absorption curves were fitted with an *n*-value of 0.5, indicating that the rate-limiting process is diffusional one-dimensional growth. Desorption curves were fitted with an *n*-value of 1.0. An *n*-value of 1 does not identify a unique rate-limiting process, but it is reasonable to believe that diffusion is the rate-limiting process for desorption. Fig. 9 gives the reaction rate constant *k* for absorption and desorption curves for samples before and after HEBM, and HEBM with and without Nb_2O_5. The *k*-values display the same trend both for absorption and desorption; highest values for ball milled samples without added Nb_2O_5, and lowest values for samples without HEBM. Table 1 gives an overview of the times needed to absorb 4 and 4.5 wt.% hydrogen. From this table, the reaction rates are slower for the 2× ECAP sample than for the as-cast alloy. However, 8× ECAP has given an improvement on the hydrogen absorption and desorption kinetics, the time to absorb respectively 4 and 4.5 wt.% H is respectively 2.5 and 3.5 min shorter for the ECAPed material than for the as-cast alloy. An explanation might be deduced from the microstructural development of the material. An eutectic alloy consists of lamellae of primary and secondary phases, where long continuous boundaries between primary and secondary phases may have a certain positive effect on the hydrogenation since they act as continuous diffusion paths. In the 2× ECAP material, the as-cast lamellae structure is partly destroyed, the microstructure is still inhomogeneous and not maximally refined, and this may result in a reduced catalytic effect for hydrogen dissociation and diffusion. In the 8× ECAP material, however, the microstructure with evenly distributed small spherical particles is fully developed, and the diffusion properties are modified optimally. In addition, there can also have been an increase in the dislocation density and/or a refinement of the matrix grain size from 2× to 8× ECAP, giving a positive effect on the diffusion properties. The obtained result is in good accordance with general theory that a higher number of ECAP presses gives a higher imposed strain and consequently increased refinement of the microstructure [13–16]. The present results are also in agreement with the data reported by Skripnyuk et al. [2] who found that a Mg/Mg_2Ni alloy processed by 10 ECAP presses absorbed 80% of the full H-storage capacity faster than the corresponding as-cast alloy.

TDS measurements were done for every sample applying a heating rate of 0.5 °C/min. Fig. 10 shows TDS traces for the 2× ECAP alloy before and after HEBM with and without added Nb_2O_5. A pronounced shift of the desorption peak towards lower temperatures is seen for all ball milled samples. Lowering of the position of the desorption peak can be explained by much smaller particle sizes and disordering of the microstructure after HEBM. Desorption starts at 130 °C for all samples. This temperature is remarkably low for an Mg-based alloy and shows that Ni and Mm gives good catalytic effects on the desorption reaction. No distinct difference between the TDS graphs of the ECAPed and as-cast samples were observed. The TDS-graphs for the samples that had been milled with Nb_2O_5 additions have the same shape and the same starting and peak temperature as the graphs for the

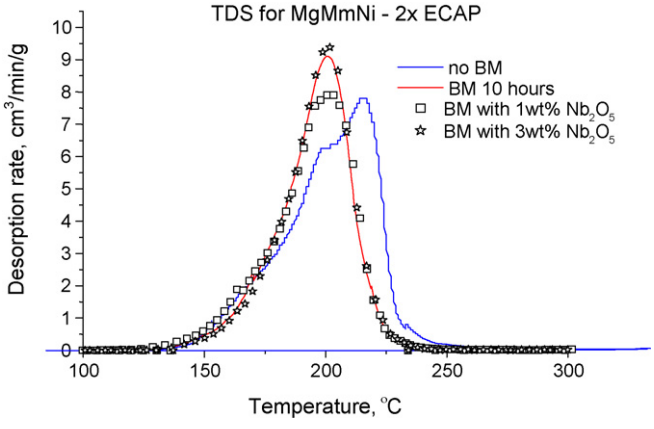

Fig. 10. Vacuum TDS traces for 2× ECAP samples.

samples that had been ball milled without Nb_2O_5 additions. This confirms that the addition of Nb_2O_5 has no special influence on neither the absorption nor the desorption properties of the Mg–Mm–Ni alloy.

4. Conclusions

The influence of alloying magnesium with nickel and Mischmetal on hydrogen-absorption behaviour has been studied in detail. Refinement of the as-cast microstructure was performed by ECAP and HEBM.

Eight ECAP passes at 400 °C gave an improvement in the hydrogen absorption and desorption rates. HEBM gave an even larger improvement and reduced the absorption and desorption times to one third of those of the as-cast alloy.

Milling of the Mg–Mm–Ni alloy under 40 bar H_2 (0.5–2 h) resulted in dramatic improvements compared to the initially non-activated samples. After HEBM in H_2, almost complete hydrogenation of the alloy was achieved during the first cycle with formation of a nanocrystalline mixture of $Mg_2NiH_{0.3}$, MgH_2 and Mg_2NiH_4.

The rates of formation and decomposition of the Mg_2NiH_4 phase are 50–150 times slower than those of the MgH_2 phase. However, formation of α-$Mg_2NiH_{0.3}$ plays a prominent role in reaching complete hydrogenation and in reaching high rates of H uptake and release. Mg_2Ni works as a catalyst and as a medium for fast exchange of hydrogen.

HEBM has a more substantial effect on hydrogen absorption–desorption kinetics of Mg–Mm–Ni than ECAP has.

Adding Nb_2O_5 as a metal oxide catalyst during HEMB gives no further improvement of the hydrogen sorption/desorption properties, indicating that the catalytic effect of metal oxide is already introduced by Mm and Mg_2Ni.

Acknowledgement

The authors wish to thank Nordic Energy Research (project NORSTORE) and Norwegian Research Council for the support.

References

[1] V.M. Skripnyuk, E. Rabkin, Y. Estrin, R. Lapovok, Acta Mater. 52 (2004) 405–414.
[2] V.M. Skripnyuk, E. Buchman, E. Rabkin, Y. Estrin, M. Popov, S. Jorgensen, J. Alloys Compd. 436 (2007) 99–106.
[3] R. Janot, F. Cuevas, M. Latroche, A. Percheron-Guégan, Intermetallics 14 (2006) 163–169.
[4] G. Barkhordarian, T. Klassen, R. Bormann, Scr. Mater. 49 (2003) 213–217.
[5] N. Hanada, T. Ichikawa, H. Fujii, J. Alloys Compd. 404/406 (2005) 716–719.
[6] J.C. Werenskiold, Equal channel angular pressing (ECAP) of AA6082: mechanical properties, texture and microstructural development, Doctoral Theses at NTNU, 2004, 129, pp. 69–73.
[7] A. Karty, J. Grunzweig-Genossar, P.S. Rudman, J. Appl. Phys. 50 (1979) 7200–7209.
[8] R.B. Von Dreele, A.C. Larson, General Structure Analysis System, Regents of the University of California, 2001.
[9] S. De Negri, M. Giovannini, A. Saccone, J. Alloys Compd. 397 (2005) 126–134.
[10] W. Oelerich, T. Klassen, R. Bormann, J. Alloys Compd. 315 (2001) 237–242.
[11] B. Vigeholm, J. Kjølner, B. Larsen, J. Less-Common Met. 74 (1980) 341–350.
[12] V.A. Yartys, M.V. Lototsky, J.P. Maehlen, Hydrogen storage in magnesium-based materials, a review, ENSYS, IFE 2005.
[13] Encycl. Mater. Sci. Technol. (2001) 3953–3970.
[14] N.E. Tran, S.G. Lambrakos, M. Ashraf Imam, J. Alloys Compd. 407 (2006) 240–248.
[15] K. Tanaka, Y. Kanda, M. Furuhashi, K. Saito, K. Kuroda, H. Saka, J. Alloys Compd. 293/295 (1999) 521–525.
[16] M. Pezat, B. Darriet, P. Hagenmuller, J. Less-Common Met. 74 (1980) 427–434.